Supporting Information

Kwon et al.

SI Materials and Methods

Generation of transgenic fly lines

Three SCA3 structural variants (*MJD*/*SCA3* variants, *MJDtr-76Q*, *MJDtr-70Q_cc0*, and *MJDtr-70Q_pQp*) were synthesized from Biomatik (Canada) and incorporated at the same attP locus (VK00033) to ensure the equal expression efficiency.

For the generation of two Foxo mutants, the structure-guided mutagenesis used in the previous study (1) was adopted. Coiled-coil structures were reported to be composed of heptad repeats (*a*-*b*-*c*-*d*-*e*-*f*-*g*), and hydrophobic residues, *a* and *d*, were shown to be responsible for shaping coils (2, 3). Therefore, two coiled-coil domains near the C-terminal regions of Foxo (Fig. S2*C*) were manipulated accordingly. For Foxo-G mutant, the *a*/*d*/*g* residues of the heptad repeats in two coiled-coil domains were replaced with glycines (Gs) (Fig. 4*A*) that are known as coiled-coil breakers (4, 5). Two coiled-coil domains of Foxo were completely deleted in the Foxo-Del mutant.

For screening experiments, *UAS-Kay-2xFlag* was generated from the LD16083 clone from BDGP and incorporated into the pACU2 vector. All these transgenic fly lines were generated at BestGene Inc. (U.S.A.).

Confocal microscope imaging

All images were acquired using LSM700 or LSM 780 confocal microscopes. Live imaging of da neurons was performed at 200x magnification, and images of samples after

immunohistochemistry experiments were taken at 400x magnification. All images of da neurons were acquired from abdominal segments A4-A6. For Thioflavin S staining experiments, using the LSM 780 confocal microscope, an excitation wavelength of 458 nm and an emission wavelength of 484-707 nm were used.

Immunohistochemistry

Immunostaining of third instar larvae was performed as described in a previous protocol (6). The following primary antibodies were used for detecting polyQ protein and its target proteins: Rat anti-HA (3F10, Roche; 1:1000 dilution) for detecting the HA epitope; mouse anti-GFP (3E6, Thermo Scientific; 1:400 dilution) for detecting GFP; mouse anti-V5 (R960-25, Thermo Scientific; 1:100 dilution) for detecting the V5 epitope; mouse anti-Flag (1E6, Wako, 1:200) for detecting the Flag epitope; and goat anti-HRP cy3 (Jackson Immunoresearch Laboratories; 1:200 dilution). Then, the following secondary antibodies were used to detect the primary antibodies: donkey anti-mouse cy3 (Jackson Immunoresearch Laboratories; 1:200 dilution); donkey anti-mouse Alexa 488 (1:1000 dilution); and goat anti-rat Alexa 647 (Jackson Immunoresearch Laboratories; 1:1000 dilution).

Thioflavin S staining

Thioflavin S staining of adult fly brains was performed as previously described (7), with a few modifications. The 50% ethanol containing 0.125% Thioflavin S (0.125% Thioflavin S staining solution, T-1892, Sigma-Aldrich) was prepared in advance after filtration with a 0.2-μm syringe. Adult fly heads (at day 5 after eclosion) were dissected in 1X PBS and fixed in 1X PBS containing 4% formaldehyde and 0.5% Triton X-100. After 2 hour fixation at

room temperature (25°C), the samples were briefly washed with 1X PBS containing 0.1% Triton X-100 (0.1% PBT). Next, the samples were incubated in 0.125% Thioflavin S staining solution overnight at 4°C. Subsequently, the samples were washed with 50% ethanol for 10 minutes, followed by successive washing with 0.1% PBT. Then, the samples were mounted in 1X PBS for confocal imaging.

Nuclear extraction and Western blot

Nuclear extraction was performed using NE-PER Nuclear and Cytoplasmic Extraction Reagents (#78835, Thermo Scientific). For this experiment, fly head samples were collected at 3 days after eclosion, and extraction procedures were followed according to the manufacturer's standard protocol.

After nuclear extraction experiment using fly head samples, Laemmli sample buffer (#161-0747, Bio-Rad) and β-mercaptoethanol were added into the nuclear extracts to be each 1 X and 2.5%, respectively. The mixtures were boiled for 5 minutes at 95°C and loaded onto Mini-PROTEAN TGX Stain-Free, 4-15% gel (#BR456-8083, Bio-Rad). Tris/Glycine/SDS buffer (#161-0732, Bio-Rad) was used as running buffer, and after electrophoresis, the proteins within the gel were transferred to the nitrocellulose membrane (#BR170-4270, Bio-Rad) in Trans-Blot® Turbo™ 5x Transfer Buffer (Bio-Rad). Prior to the primary antibody incubation, the nitrocellulose membrane was incubated in the blocking buffer composed of TBST (50 mM Tris-HCl pH 7.4, 150 mM NaCl, and 0.1% Tween-20) containing 5% skim milk. To detect HA-tagged polyQ proteins, rat anti-HA (3F10, Roche; 1:1000 dilution) was used. Rabbit anti-Histone 3 (Ab1791, Abcam; 1:1000 dilution) was used as a control. All primary antibody incubations were performed overnight at 4°C. After overnight incubation, the membrane was washed several times with TBST for 25 minutes. Then, the membrane was incubated in the

blocking buffer containing the secondary antibodies, goat anti-rat HRP conjugated (sc-2006, Santa Cruz; 1:3000) and goat anti-rabbit HRP conjugated (sc-2004, Santa Cruz; 1:3000), for one hour at room temperature (25°C). Several washing steps were performed with TBST for 25 minutes prior to detection with enhanced chemiluminescence (#BR170-5060, Bio-Rad) in ChemiDoc™ XRS+.

Selection of TF list

To identify the interactors of SCA3 polyQ proteins, we first collected 294 trusted TFs which were experimentally verified or predicted to have canonical DNA-binding domains according to the information at FlyTF.org (8). We further narrow them down to 58 TFs that are annotated with the GOBP term of 'dendrite morphogenesis' in AmiGO database (ver. 1.8) (9) and/or were reported to be associated with dendrite morphogenesis in previous studies. For each of these 58 TFs, COILS program with a 21-amino-acid scanning window (10) was used to compute the probability that it forms coiled-coil structures. Finally, 13 TFs with at least one region containing amino acid sequences with the probability larger than 0.9 were selected for further screening (Table 1).

Co-immunoprecipitation (co-IP)

Co-IP experiments were performed as previously described (6). After preparation of protein lysates from adult fly heads, same amounts of total proteins were incubated with 1μg of anti-V5 antibody (R960-25, Thermo Scientific) or 1μg of anti-Flag antibody (1E6, Wako) at 4°C overnight. Then, pre-cleaned protein A/G plus-agarose beads (sc-2003, Santa Cruz) were co-incubated for 3 hours at at 4°C shaking incubator. After the incubation, the agarose beads

were precipitated and washed with lysis buffer (150mM NaCl, 1% Triton X-100, 50mM Tris-HCl pH7.5) for 3 times. The immunoprecipitated lysates were eluted in 1x Laemmle buffer (#161-0747, Bio-Rad) containing 2.5% β-mercaptoethanol.

RNA extraction and RT-PCR

RT-PCR analysis was performed as previously described (6). Fly head samples were collected at 3 days after eclosion, and total RNAs were extracted using easy-Blue system (iNtRON Biotechnology, Korea). We used 3μg of total RNAs for cDNA synthesis using GoScript™ Reverse Transcriptase with the manufacturer's standard protocol (A2791, Promega). RT-PCR was performed using C1000™ Thermal Cycler, C1000 Touch™ Thermal Cycler or T100™ Thermal Cycler system (Bio-Rad) with the following cycles: *Kay* (26), *Xnp* (25), *Dad* (27), *Khc* (26), and *Snana* (25).

Table S1. Primers for RT-PCR analysis

Gene	**Sequences**
Kay	5'-ACACGACCGATACTTCAAGTGC 3'-CCAGAAGGTACTCCAGCTGATTCT
Dad	5'-ATTTCGCGAGGATTTCGAAGCG 3'-GCGGTGTTGGGGATTCTGTTT
Xnp	5'-TTGACGAGGAGTCGAAAAAGGC 3'-GGGCTTGTCCTTATAGCGTGAGA
Khc	5'-GCATATCCATAGCGGGCAAGGTG

	3’-AGTTCACCTTGGAGACGTCCAACAG
Snama	5’-GCCCAGCAAAAGATCCCCCAGTTA 3’-ATTCATACCTCCGCCTGCAGATCC

Larval motility assay

The third instar larvae expressing denoted transgenes tested in da neuronal clusters using *109(2)80*-gal4 driver were used for all motility assays. Prior to the motility assay, each larva was briefly washed in 1x PBS and placed in the center of a 90-mm Petri dish. The 90-mm Petri dish and larvae were placed inside a dark box equipped with indirect lighting. After a brief recovery time of 30 seconds, for each genotype, we recorded the times for the larvae ($N \geq 20$ per genotype) to reach the edge of the Petri dish for up to 100 seconds in an $N \times 1$ vector. We then estimated a cumulative density function for the recorded times by applying the Gaussian kernel density estimation method (11). Next, we evaluated the statistical significance of the difference between the cumulative density function of two different genotypes (G1 and G2) using the following procedure. We first combined the recorded times for G1 ($N_1 \times 1$) and G2 ($N_2 \times 1$) into a $(N_1 + N_2) \times 1$ vector, randomly permuted the elements in the combined vector, split the permuted vector into $G1_{rand}$ ($N_1 \times 1$) and $G2_{rand}$ ($N_2 \times 1$), estimated cumulative density functions for $G1_{rand}$ and $G2_{rand}$, and then computed the maximum difference (K-S statistic) between the two cumulative density functions. The random permutation was repeated 100,000 times, resulting in 100,000 random K-S statistic values. Second, an empirical null distribution for the K-S statistic value was estimated by applying the Gaussian kernel density estimation method (11) to the 100,000 random K-S statistic values. Third, the P-value for the observed K-S statistic value (Fig. 5*B*, and Fig. S4*C*) was computed by the right-sided test using the empirical distribution. These steps were applied to all pairs of genotypes tested.

EthoVision XT

After performing the motility assay for each larva, EthoVision XT (11.5 version; Noldus Information Technology, Wageningen, Netherlands) video tracking system (12) was used to further analyze the acquired video files (mp4 files). The trace of traveling larva until reaching the dish edge (up to 100 seconds) was presented using a heat map in which the color indicates a large (red) or small (blue) amount of time the larva spent in a specific location. For all heat maps, the amounts of time were normalized into those during 100 seconds. Head turning of each larva was monitored and further analyzed using *Heading* tool in EthoVision XT. The angle of head turning was defined as the angle between larval head direction and the reference line (Fig. S4*A*). Changes in head angle of each larva were calculated at every second for 1 minute.

Analysis for larval head turning

For each genotype, we measured the head turning angle of larvae (N = 4 per genotype) at every 1 second and then sampled 60 continuous head turning angles for the four replicates, resulting in 240 head turning angles (240 × 1 vector). We then evaluated the statistical significance of the difference in the head turning angles between two different genotypes (G1 and G2) using the following procedure. We first combined the head turning angles for all the nine genotypes into a 2,160×1 vector, randomly permuted the elements in the combined vector, extracted $G1_{rand}$ (240×1) and $G2_{rand}$ (240×1) from the permuted vector, and then computed the ratio of variances (F-statistic) between $G1_{rand}$ and $G2_{rand}$. This random permutation was repeated 100,000 times, resulting in 100,000 random F-statistic values. Second, an empirical

null distribution for the F-statistic value was estimated by applying the Gaussian kernel density estimation method (11) to the 100,000 random F-statistic values. Third, the P-value for the observed F-statistic value (Fig. 5*D*) was computed by the right-sided test using the empirical distribution. To test the decrease in head turning angles by Foxo overexpression (Fig. 5*D*), we defined an F-statistic value as the ratio of the variance in the control condition to the variance in the Foxo-overexpressing condition. To test the increase in head turning angle by Foxo RNAi (Fig. S4*E*), we defined an F-statistic value as the ratio of the variance in the Foxo RNAi condition to the variance in the control condition.

A

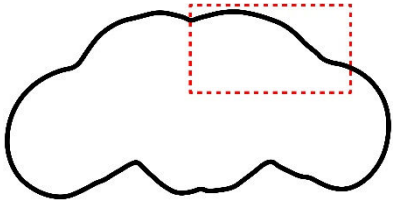

C

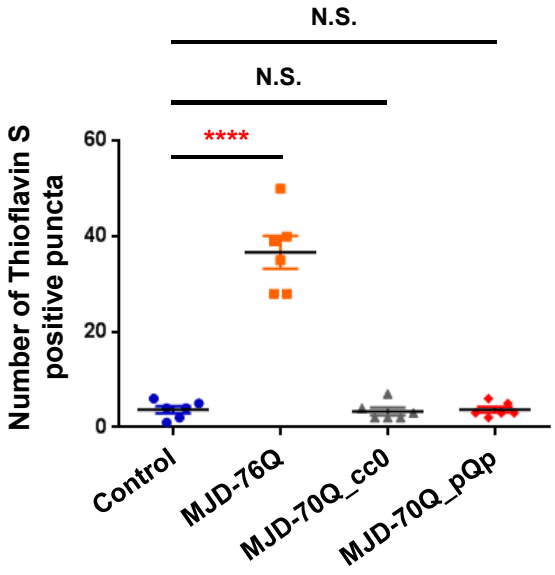

B

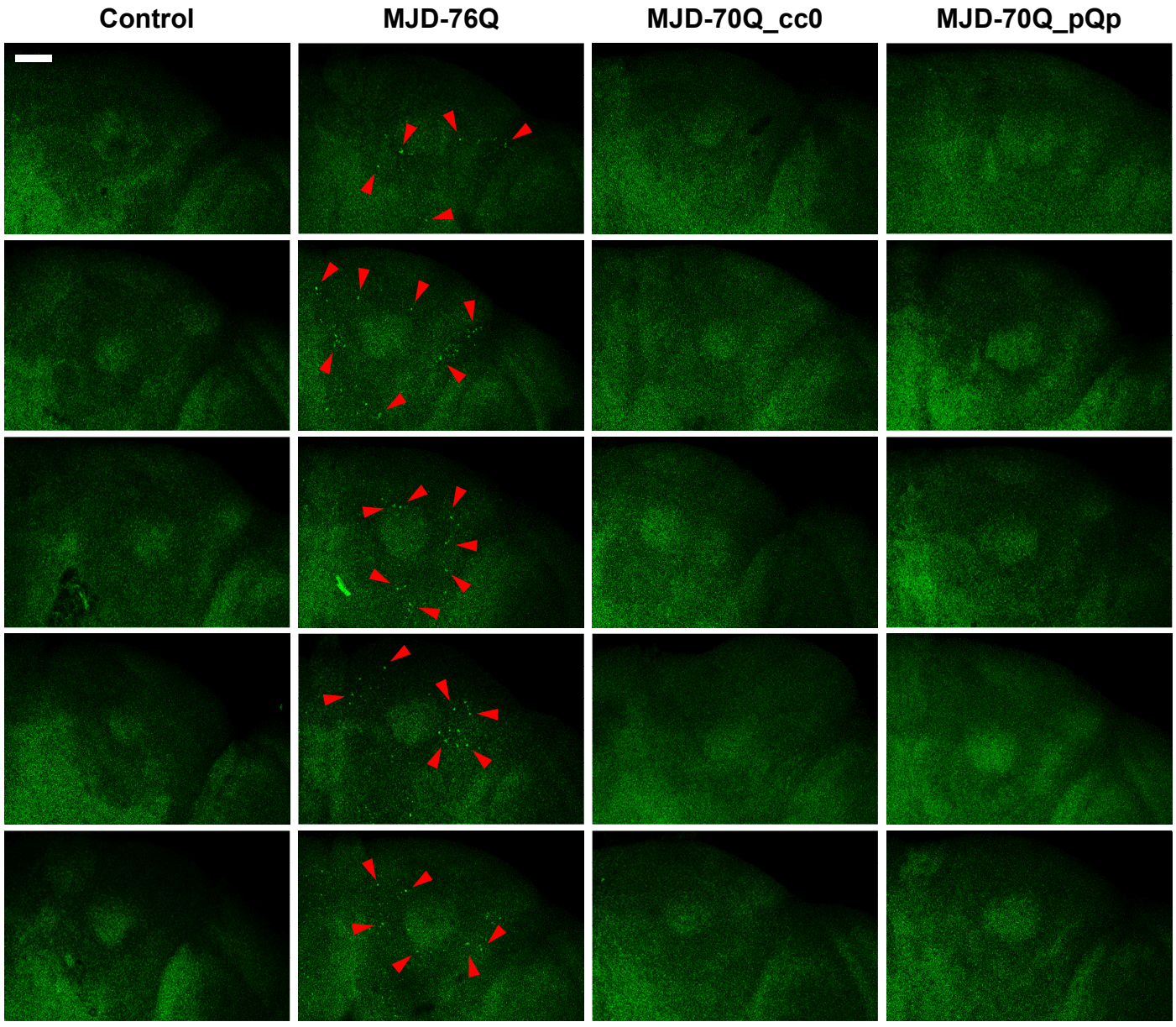

Supplementary Fig S1

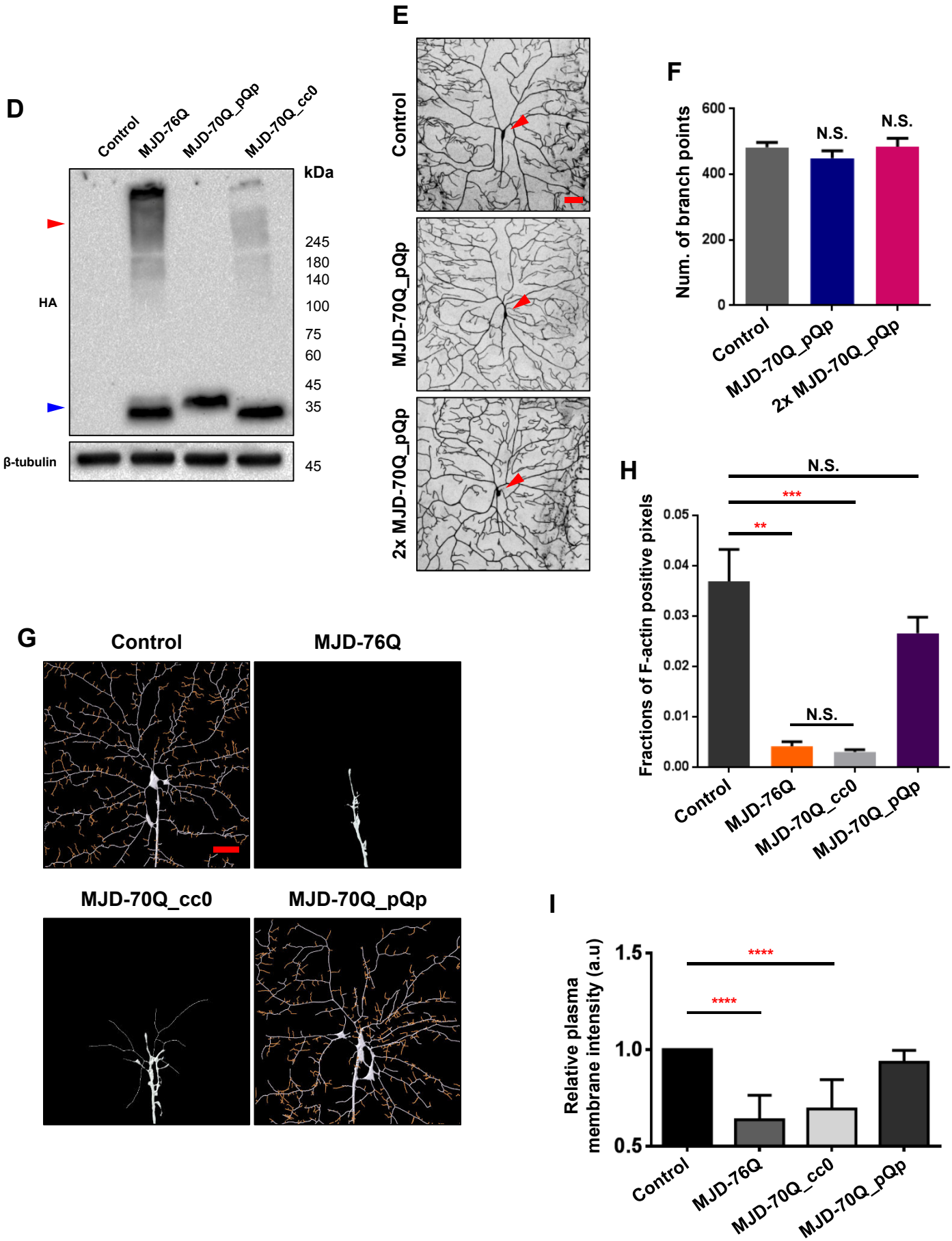

Supplementary Fig S1

Fig. S1. Coiled-coil structures of SCA3 polyQ proteins disrupt actin cytoskeletal structures and PM protein supplies.

(A) A diagram illustrating the brain region of adult fly analyzed for Thioflavin S staining experiments in (*B*) and (*C*).

(B) Magnified images of adult fly brains marked in (*A*) after Thioflavin S staining (*elav-Gal4*/+, *elav-Gal4*/*UAS-MJDtr-76Q*, *elav-Gal4*/*UAS-MJDtr-70Q_cc0*, and *elav-Gal4*/*UAS-MJDtr-70Q_pQp*). Scale bar (white), 50 μm. Arrowheads (red) indicate Thioflavin S positive puncta.

(C) Quantification of the number of Thioflavin S positive puncta in a brain region illustrated in (*A*). N.S., not significant; **** $P < 1.0 \times 10^{-4}$ by one-way ANOVA with Tukey post hoc test; error bars, SEM; n = 6 brains.

(D) Representative images obtained from Western blot analysis of whole cell lysates from adult fly heads (*elav-Gal4*/+, *elav-Gal4*/*MJDtr-76Q*, *elav-Gal4*/*MJDtr-70Q_cc0*, and *elav-Gal4*/*MJDtr-70Q_pQp*). SCA3 polyQ proteins tagged with HA epitopes were immunoblotted using anti-HA antibody. β-tubulin was used as a loading control.

(E) Dendrite images of control C4da neurons (top) and C4da neurons overexpressing MJDtr-70Q_pQp (middle) or 2x MJDtr-70Q_pQp (bottom) (*UAS-CD4td-GFP*/+;*ppk-Gal4*/+, *UAS-CD4td-GFP*/+;*ppk-Gal4/UAS-MJDtr-70Q_pQp*, and *UAS-CD4td-GFP*/+;*ppk-Gal4,UAS-MJDtr-70Q_pQp/UAS-MJDtr-70Q_pQp*). Arrowheads (red) indicate cell bodies of C4da neurons. Scale bar (red), 50 μm.

(F) Quantification of the number of dendrite branch points of C4da neurons expressing transgenes described in (*E*). N.S., not significant by one-way ANOVA with Tukey post hoc test; error bars, SEM; n = 3 neurons.

(G) Actin cytoskeletal structure images of da neuronal clusters expressing MJDtr-76Q, MJDtr-70Q_cc0, or MJDtr-70Q_pQp (*109(2)80-Gal4*/+;*UAS-GMA*/+, *109(2)80-Gal4*/+;*UAS-GMA*/*UAS-MJDtr-76Q, 109(2)80-Gal4*/+;*UAS-GMA*/*UAS-MJDtr-70Q_cc0*, and *109(2)80-Gal4*/+;*UAS-GMA*/*UAS-MJDtr-70Q_pQp*). Actin structures are represented in pseudo-color images converted by Imaris. Scale bar (red), 50 μm. n ≥ 8 da neuronal clusters.

(H) Quantified fractions of F-actin marker (GMA) positive pixels, which have non-zero GMA intensities, in each dorsal cluster da neuron expressing denoted transgenes described in (*A*). N.S. not significant; ** $P < 1.0 \times 10^{-2}$; *** $P < 1.0 \times 10^{-3}$ by one-way ANOVA with Tukey post hoc test; error bars, SEM; n ≥ 3 da neuronal clusters.

(I) Quantification of pixel intensities of plasma membrane-targeted CD4-tdGFP in C4da neurons expressing MJDtr-76Q, MJDtr-70Q_cc0, or MJDtr-70Q_pQp proteins (*UAS-CD4-tdGFP*/+;*ppk-Gal4*/+, *UAS-CD4-tdGFP*/+;*ppk-Gal4*/*UAS-MJDtr-76Q*, *UAS-CD4-tdGFP*/+;*ppk-Gal4*/*UAS-MJDtr-70Q_cc0*, and *UAS-CD4-tdGFP*/+;*ppk-Gal4*/*UAS-MJDtr-70Q_pQp*). **** $P < 1.0 \times 10^{-4}$ by one-way ANOVA with Tukey post hoc test; error bars, SEM; n = 16 neurons.

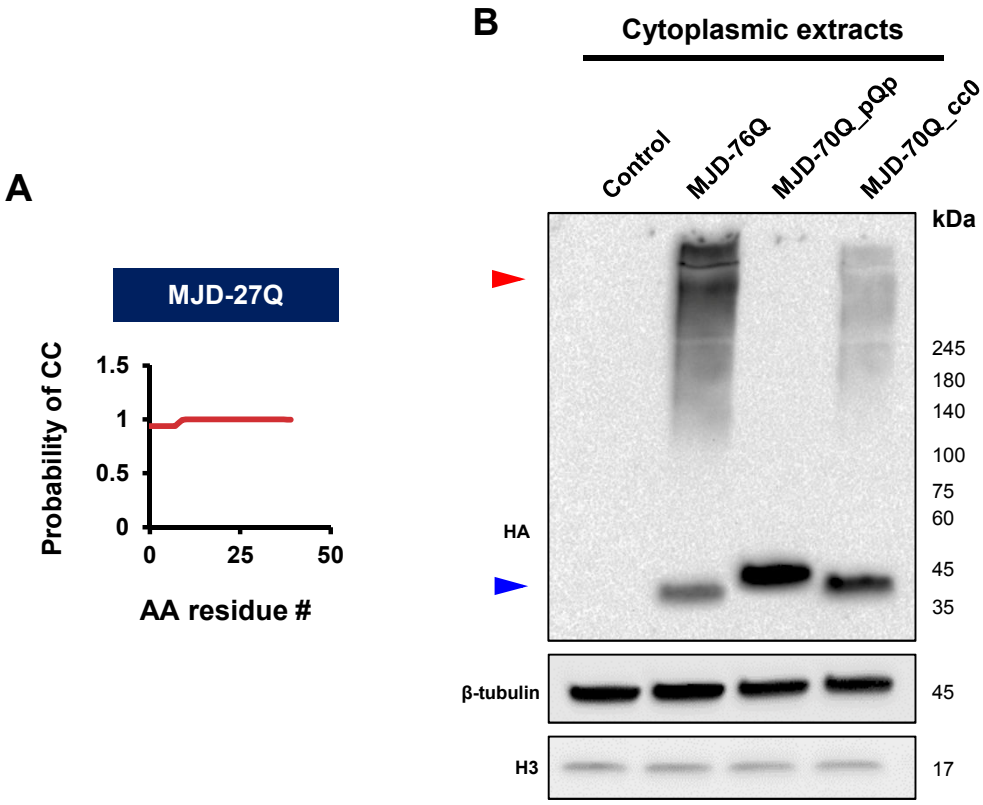

Supplementary Fig S2

Fig. S2. SCA3 polyQ proteins without coiled-coil structures are predominantly localized in cytoplasm.

(A) Probabilities to form coiled-coil structure in MJDtr-27Q calculated by COILS. *y* axis indicates the predicted probability to form coiled-coil structures, and *x* axis indicates the amino acid residue numbers.

(B) Representative images obtained from Western blot analysis of cytoplasmic lysates from adult fly heads (*elav-Gal4*/+, *elav-Gal4*/*MJDtr-76Q*, *elav-Gal4*/*MJDtr-70Q_cc0*, and *elav-Gal4*/*MJDtr-70Q_pQp*). SCA3 polyQ proteins tagged with HA epitopes were immunoblotted using anti-HA antibody. β-tubulin and histone 3 (H3) are used as the loading controls.

A

Dendrite morphogenesis-related TFs
58 TFs

Coiled coil-rich TFs
13 TFs

> 25% reduction in the number of dendrite branch points after TF knockdown
6 TFs
(Foxo, Cut, Kay, Nub, Nej, and Cnc)

> 4-fold restoration in the number of dendrite branch points after TF overexpression
3 TFs
(Foxo, Cut, and E2f1)

intersection

2 TFs selected
(Foxo and Cut)

B

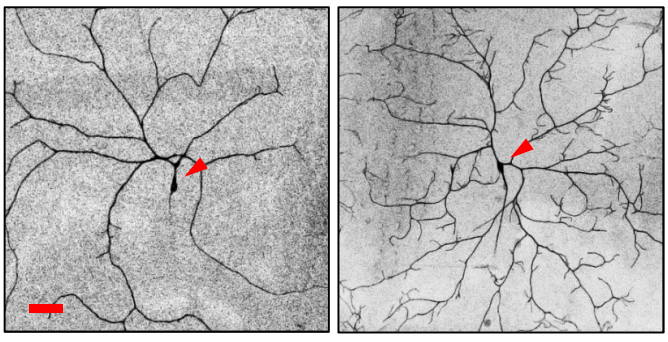

C

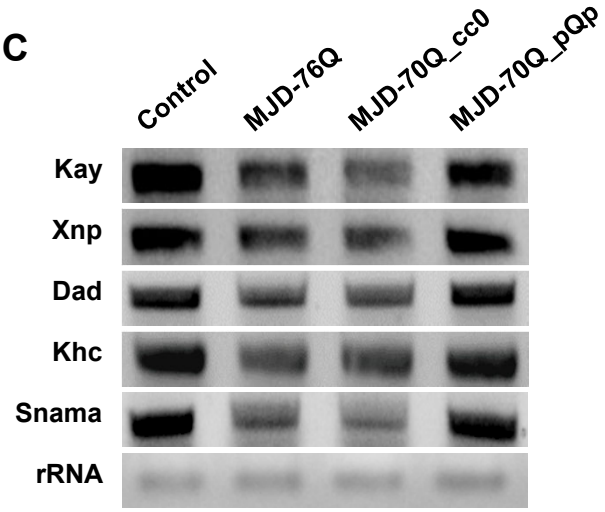

Supplementary Fig S3

Fig. S3. Coiled-coil-rich Foxo is one of the most potent interactors of SCA3 polyQ proteins

(A) Overall scheme for selection of potential transcription factors (TFs) that interact with polyQ proteins and are associated with dendrite morphogenesis.

(B) Dendrite images of C4da neurons overexpressing MJDtr-70Q_cc0 (left) or MJDtr-70Q_cc0 + Cut (right) (*UAS-CD4td-GFP*/+;*ppk-Gal4*,*UAS-MJDtr-70Q_cc0*/+ and *UAS-CD4td-GFP*/+;*ppk-Gal4*,*UAS-MJDtr-70Q_cc0*/*UAS-Cut-3xHA*). Arrowheads (red) indicate cell bodies of C4da neurons. Scale bars, 50 μm.

(C) mRNA levels of Foxo-target genes (*Kay*, *Xnp*, *Dad*, *Khc*, and *Snama*) measured by RT-PCR analysis. rRNA is used as a control.

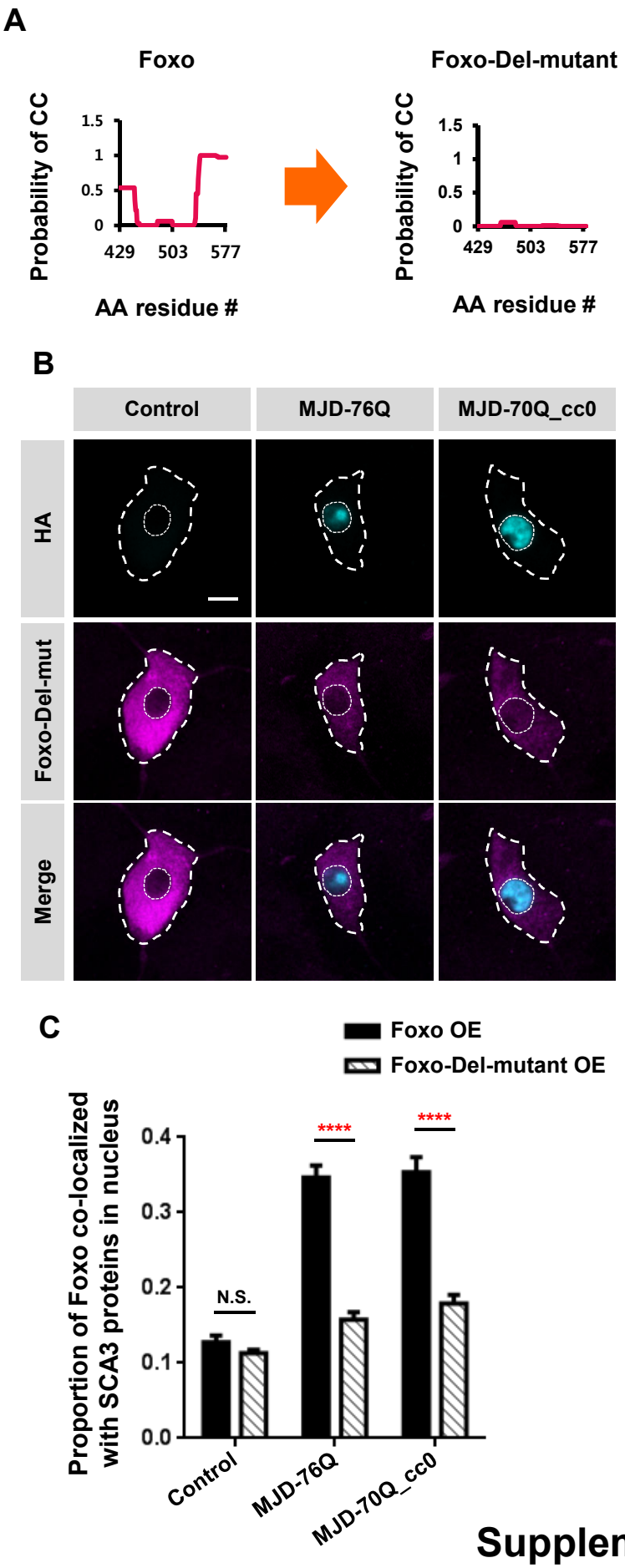

Supplementary Fig S4

Fig. S4. **Deletion of coiled-coil structures in Foxo abolishes its nuclear interactions with SCA3 polyQ proteins.**

(A) Probabilities to form a coiled-coil structure in Foxo-Del mutants calculated by COILS. *y* axes indicate the probability to form a coiled-coil structure, and *x* axes indicate the amino acid residue numbers.

(B) Subcellular localization of Foxo-Del mutants (magenta) and SCA3 structural variants (cyan in C4da neurons overexpressing Foxo-Del mutant, MJDtr-76Q + Foxo-Del mutant, or MJDtr-70Q_cc0 + Foxo-Del mutant. (*UAS-Foxo-Del mutant-Flag*/*UAS-CD4-tdGFP*;*ppk-Gal4*/+ (Control), *UAS-Foxo-Del mutant-Flag*/*UAS-CD4-tdGFP*;*ppk-Gal4*,*UAS-MJDtr-76Q*/+, and *UAS-Foxo-Del mutant-Flag*/*UAS-CD4-tdGFP*;*ppk-Gal4*,*UAS-MJDtr-70Q_cc0*/+). Outer and inner dashed lines (white) indicate the outlines of the cell body and nucleus. Scale bar, 5 μm.

(C) Comparison of nuclear proportions of wild-type Foxo and Foxo-Del mutants co-localized with SCA3 proteins in C4da neurons expressing denoted transgenes. N.S., not significant; **** $P < 1.0 \times 10^{-4}$ by two-way ANOVA with Tukey post hoc test; error bars, SEM; $n \geq 12$ neurons.

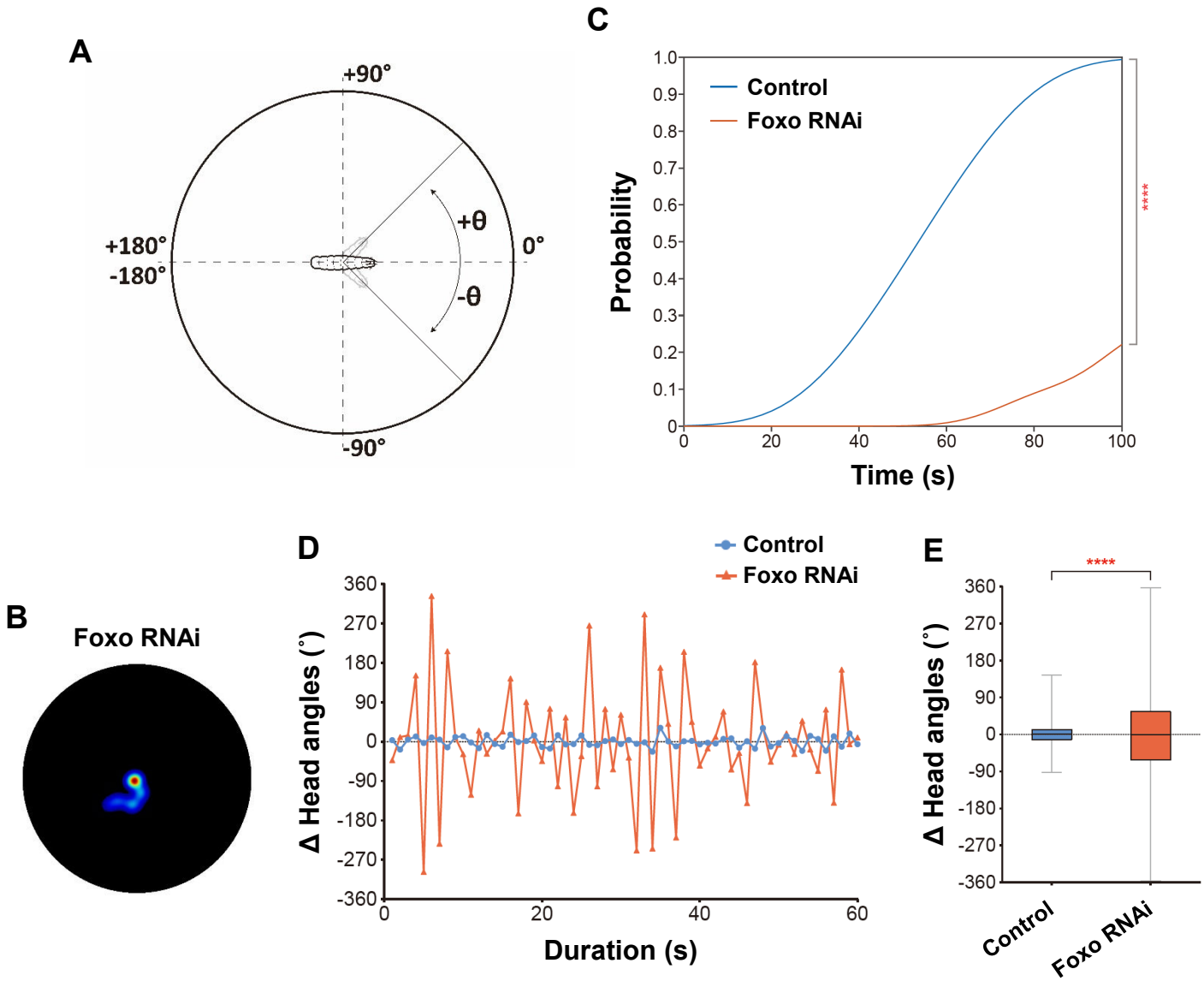

Supplementary Fig S5

Fig. S5. **Knockdown of Foxo results in impaired larval motility.**

(A) A schematic diagram illustrating how the head turning angle (θ) of the larva is defined by EthoVision XT. Turning the head to left and right is defined as positive (+θ) and negative (-θ) angles, respectively.

(B) Heat maps showing residence probability during traveling of larvae expressing Foxo RNAi (*109(2)80-Gal4*/+;*UAS-Foxo RNAi*/+).

(C) Cumulative density functions showing fractions of larvae that reach the dish edge over time (*109(2)80-Gal4*/+;+/+ and *109(2)80-Gal4*/+;*UAS-Foxo RNAi*/+). **** $P < 1.0 \times 10^{-4}$ by random permutation experiments; $n \geq 26$ independent larvae.

(D) Representative changing patterns of head angles of larvae in every second for 1 minute. Turning the head to left and right is presented as positive (+) and negative (-) angles, respectively.

(E) Box plots showing the variability of head angle changes in larvae expressing transgenes described in (*C*). **** $P < 1.0 \times 10^{-4}$ by random permutation experiments; $n = 4$ independent larvae.

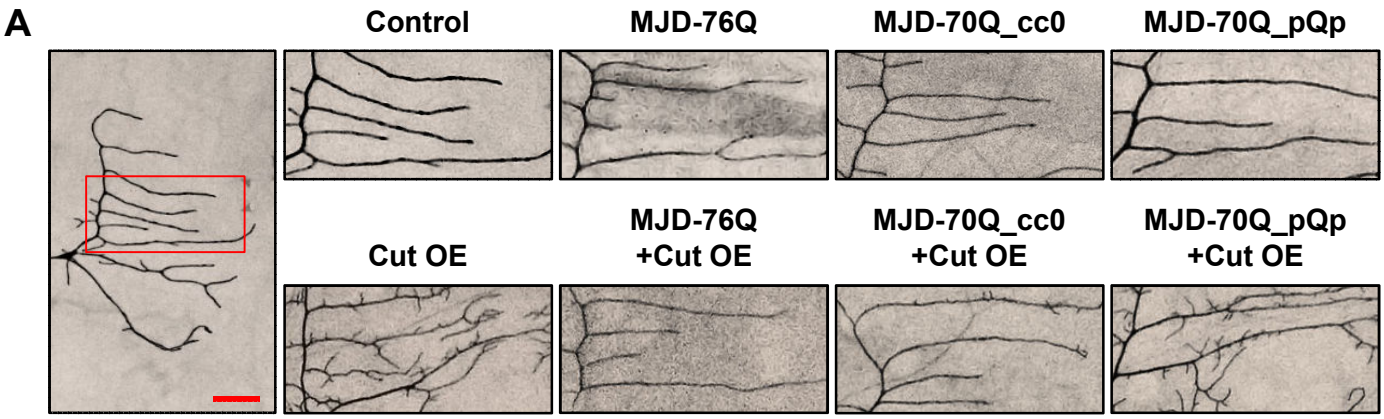

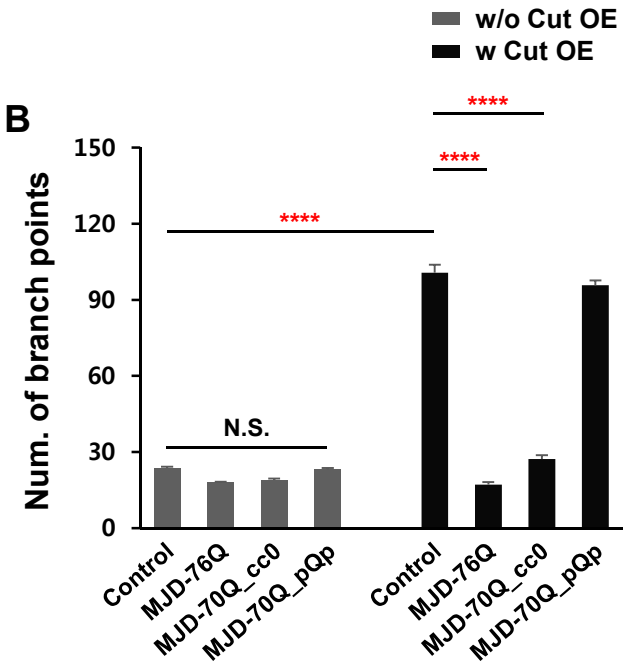

Supplementary Fig S6

Fig. S6. **Coiled-coil structures of SCA3 polyQ proteins are crucial for their genetic inhibition of Cut functions in C1da neurons.**

(A) Dendrite images of C1da neurons expressing denoted transgenes (*221-Gal4*,*UAS*-m*CD8-GFP*/+, *221-Gal4*,*UAS*-m*CD8-GFP*/*UAS-MJDtr-76Q*, *221-Gal4*,*UAS*-m*CD8-GFP*/*UAS-MJDtr-70Q_cc0*, *221-Gal4,UAS*-m*CD8-GFP*/*UAS-MJDtr-70Q_pQp*, *UAS-Ct*/+;*221-Gal4*,*UAS*-m*CD8-GFP*/+, *UAS-Ct*/+;*221-Gal4*,*UAS*-m*CD8-GFP*/*UAS-MJDtr-76Q*, *UAS-Ct*/+;*221-Gal4*,*UAS*-m*CD8-GFP*/*UAS-MJDtr-70Q_cc0*, and *UAS-Ct*/+;*221-Gal4*,*UAS*-m*CD8-GFP*/*UAS-MJDtr-70Q_pQp*). The region in the red square of left panel is magnified in the dendrite image of a C1da neuron expressing each transgene. Scale bar (red), 50 μm.

(B) Quantification of the number of dendrite branch points of C1da neurons expressing transgenes described in (*A*). N.S., not significant; **** $P < 1.0 \times 10^{-4}$ by two-way ANOVA with Tukey post hoc test; error bars ± SEM; n = 15 neurons.

References

1. Fiumara F, Fioriti L, Kandel ER, & Hendrickson WA (2010) Essential role of coiled coils for aggregation and activity of Q/N-rich prions and PolyQ proteins. *Cell* 143(7):1121-1135.
2. Monera OD, Zhou NE, Lavigne P, Kay CM, & Hodges RS (1996) Formation of parallel and antiparallel coiled-coils controlled by the relative positions of alanine residues in the hydrophobic core. *Journal of Biological Chemistry* 271(8):3995-4001.
3. Oakley MG & Hollenbeck JJ (2001) The design of antiparallel coiled coils. *Curr Opin Struc Biol* 11(4):450-457.
4. Surkont J & Pereira-Leal JB (2015) Evolutionary patterns in coiled-coils. *Genome Biol Evol* 7(2):545-556.
5. Lupas AN & Gruber M (2005) The structure of alpha-helical coiled coils. *Adv Protein Chem* 70:37-78.
6. Chung CG, *et al.* (2017) Golgi Outpost Synthesis Impaired by Toxic Polyglutamine Proteins Contributes to Dendritic Pathology in Neurons. *Cell Rep* 20(2):356-369.
7. Lee S, *et al.* (2016) The calcineurin inhibitor Sarah (Nebula) exacerbates Abeta42 phenotypes in a Drosophila model of Alzheimer's disease. *Dis Model Mech* 9(3):295-306.
8. Adryan B & Teichmann SA (2006) FlyTF: a systematic review of site-specific transcription factors in the fruit fly Drosophila melanogaster. *Bioinformatics* 22(12):1532-1533.
9. Gene Ontology C (2015) Gene Ontology Consortium: going forward. *Nucleic Acids Res* 43(Database issue):D1049-1056.
10. Lupas A, Van Dyke M, & Stock J (1991) Predicting coiled coils from protein sequences. *Science* 252(5009):1162-1164.
11. Bowman AW & Azzalini A (1997) *Applied smoothing techniques for data analysis : the kernel approach with S-Plus illustrations* (Clarendon Press ;Oxford University Press, OxfordNew York) pp xi, 193 p.
12. Noldus LP, Spink AJ, & Tegelenbosch RA (2001) EthoVision: a versatile video tracking system for automation of behavioral experiments. *Behav Res Methods Instrum Comput* 33(3):398-414.